Journal of Power Sources 196 (2011) 6382–6387

Contents lists available at ScienceDirect

Journal of Power Sources

journal homepage: www.elsevier.com/locate/jpowsour

In situ scanning electron microscopy on lithium-ion battery electrodes using an ionic liquid

Di Chen[a], Sylvio Indris[b], Michael Schulz[c], Benedikt Gamer[a], Reiner Mönig[a,*]

[a] Karlsruhe Institute of Technology, Institute for Applied Materials – Materials and Biomechanics, Postfach 3640, 76021 Karlsruhe, Germany
[b] Karlsruhe Institute of Technology, Institute for Nanotechnology, Postfach 3640, 76021 Karlsruhe, Germany
[c] Karlsruhe Institute of Technology, Institute for Applied Materials – Materials Processing Technology, Postfach 3640, 76021 Karlsruhe, Germany

ARTICLE INFO

Article history:
Received 14 December 2010
Received in revised form 1 April 2011
Accepted 3 April 2011
Available online 8 April 2011

Keywords:
Lithium-ion battery
In situ electron microscopy
Ionic liquid
Tin dioxide

ABSTRACT

We present an experimental platform that can be used for investigating lithium-ion batteries with very high spatial resolution. This *in situ* experiment runs inside a scanning electron microscope (SEM) and is able to track the morphology of an electrode including active and passive materials in real time. In this work it has been used to observe SnO_2 during lithium uptake and release inside a working battery electrode. The experiment strongly relies on an ionic liquid which has very low vapor pressure and can therefore be used as an electrolyte inside the vacuum chamber of the SEM. In contrast to common electrochemical characterization tools, this method allows for the observation of microscopic mechanisms in electrodes. Depending on the SEM, resolutions down to 1 nm can be achieved. As a result, the experimental platform can be used to investigate chemical reaction pathways, to monitor phase changes in electrodes or to investigate degradation effects in batteries. SnO_2 is a potential anode material for future high capacity lithium-ion batteries. Our observations reveal the formation of interface layers, large volume expansions, growth of extrusions, as well as mechanically induced cracks in the electrode particles during cycling.

1. Introduction

Currently, rechargeable lithium-ion batteries are promising systems for the storage of energy in many applications. Lithium-ion batteries have high energy densities making them favorable for future applications such as full electric vehicles and for the storage of electrical energy from fluctuating sources like wind and solar energy. During charge and discharge, lithium ions migrate between two electrodes and react with the electrode materials. Details of these reactions and their consequences are critical to the performance and reliability of batteries.

In order to be able to charge and discharge batteries with reasonable rates, sufficient ionic and electronic conductivities are needed. Since the intrinsic electronic and ionic conductivities of the electrochemically active materials are often quite low, small particles with a high surface area are used. This results in a large interfacial area between electrolyte and the particles and short electrical paths inside the particles. Both effects are advantageous for the specific power of a battery. Depending on the material, typical electrode particles have sizes between several tens of nanometers up to a few micrometers. Battery electrodes are produced by embedding particles of the electrochemically active material within a porous matrix consisting of a polymeric binder and carbon particles for enhancing electrical conductivity. During insertion and extraction of lithium in the electrodes, many different chemical and physical reactions can occur. Typically new battery materials are examined by cyclic voltammetry which can only give spatial averages of the battery behavior and does not account for the local aspects that occur inside a battery. Also other commonly employed methods as electrochemical impedance spectroscopy or *in situ* X-ray diffraction can only be used to monitor spatial averages of an electrode.

Since electrode materials are inherently nanoscale materials, local observations of these materials in high resolution can be helpful to understand the microscopic processes that occur inside nanoparticles and at their interfaces with the electrolyte. *In situ* optical microscopy of the electrode materials has been carried out by several groups [1–3]. However, the resolution of optical microscopes is rather limited and is often too low for most of the nanoscale materials. Scanning electron microscopy (SEM) offers a much higher resolution but is difficult to perform on a working battery due to the vacuum that is needed and the presence of high energy electrons which can interfere with the battery operation. In most SEM investigations of lithium batteries [4,5], batteries had to be dismantled and the electrolyte had to be removed before they were observed. Risks of damage and contamination exist and extreme care must be taken to keep the battery materials away

* Corresponding author. Tel.: +49 721 608 22487; fax: +49 721 608 22347.
E-mail address: reiner.moenig@kit.edu (R. Mönig).

0378-7753/$ – see front matter © 2011 Elsevier B.V. All rights reserved.
doi:10.1016/j.jpowsour.2011.04.009

from atmosphere or moisture where they would be altered by the reactions with oxygen, nitrogen or water [6].

Other attempts of *in situ* SEM battery experiments have been pursued by several groups [7–9]. In the following, the different concepts for SEM observations will be briefly discussed. Baudry and Armand [7] used a polymeric electrolyte. Because of the low ionic conductivity, the batteries had to be heated to achieve reasonable cycling rates. This influence of heating on the battery performance could not be investigated. Furthermore, during the transfer process to the vacuum chamber of the SEM, the battery was in contact with the atmosphere for about 30 s. Orsini et al. [8] used an electrolyte that is commonly employed in commercial batteries consisting of ethylene carbonate/dimethyl carbonate solution with 1 M $LiPF_6$ salt. After a given number of cycles the batteries were cooled to −20 °C to freeze the electrolyte and then transferred into the SEM under protective atmosphere. Contamination could be prevented by doing this but the batteries could not be electrically cycled inside the SEM. Another interesting approach was taken by Raimann et al. [9] who used carbonate solvents (ethylene carbonate and propylene carbonate) with high boiling point as an electrolyte in an *in situ* environmental scanning electron microscope (ESEM). ESEMs allow the imaging of samples with higher vapor pressures. In certain cases even wet samples can be imaged. Unfortunately, the resolution of such SEMs is reduced due to scattering of electrons in the gas atmosphere that is present inside the SEM chamber. Since the electrolyte evaporated, experiments had to be carried out quickly in this study.

In this work we used a room temperature ionic liquid (IL) based electrolyte in our test cell inside a standard SEM. ILs are currently discussed as possible electrolytes for future batteries [10]. They are chemically very stable and offer enhanced safety for batteries [11]. ILs are room temperature molten salts based on organic anions and cations that exhibit extremely low vapor pressures and can even be used under ultra high vacuum conditions. This makes them ideal for many experiments, where vacuum compatibility is needed. In the experiments that are presented here, an IL was combined with lithium and SnO_2 to build batteries. With this configuration it is possible to perform detailed microscopic studies on batteries. Here we present data obtained on SnO_2 which was used as an example material. SnO_2 has a high capacity for lithium and is a candidate material for future anodes in lithium-ion batteries. During its reaction with lithium, SnO_2 is reduced to Sn metal (Eq. (1)). Sn further reacts with lithium by alloying where alloys with Li_xSn with $0 \leq x \leq 4.4$ from (Eq. (2)).

$$\text{Step 1}: \quad 4Li + SnO_2 \rightarrow 2Li_2O + Sn \tag{1}$$

$$\text{Step 2}: \quad xLi + Sn \leftrightarrow Li_xSn\,(0 \leq x \leq 4.4) \tag{2}$$

The second reaction step (Eq. (2)) is reversible and Sn therefore can be used as an electrode material for reversible lithium ion storage. Sn has a fairly low voltage against lithium and a large theoretical capacity of 991 mAh g^{-1} [12]. This capacity is almost three times that of graphite, today's standard material. Sn would be an ideal anode material for batteries if there were no detrimental processes associated with its reaction. Unfortunately, the alloying process is accompanied by a large volume expansion where the volume increases by a factor of 3.6 and a rather poor reliability of this material has been reported [13]. Besides other effects, large volume expansions can induce mechanical stresses and crack initiation in the electrode. Consequently, the conductivity of the electrode is reduced, the capacity decreases and the internal resistance increases, which could result in poor cycling stability. One option to increase the cycle life of electrodes is to use SnO_2 as a starting material. In an initial reaction the oxygen from the SnO_2 reacts with lithium to form an amorphous Li_2O matrix and elementary Sn (Eq. (1)). It is suspected that Sn is finely distributed in the form of particles inside the Li_2O matrix. This matrix may help to distribute

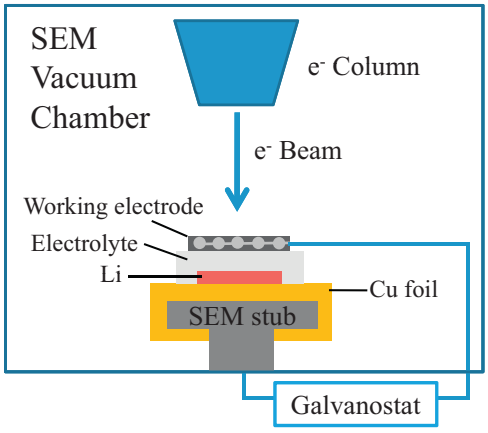

Fig. 1. Setup of the lithium-ion cell for the *in situ* experiment in the SEM. Using a mesh as current collector allows permeation of electrolyte and the imaging of the electrode.

stresses that occur in the Sn particles during alloying. It has been speculated that the Li_2O matrix improves the cycling stability of the electrode by preventing the Sn metal particles from agglomerating. Once significantly large Sn entities are formed, the large volume changes may induce sufficient stresses to damage the matrix [12]. The theoretical capacity of SnO_2 of the first discharge based on formation of Li_2O and lithium alloying in Sn is 1491 mAh g^{-1} [12]. The theoretical capacity of the second discharge of SnO_2 based on lithium alloying is 781 mAh g^{-1}. The second discharge capacity is assumed to be reversible. The observed capacity is commonly much smaller than the theoretical value and decreases quickly after several cycles. In this work, *in situ* SEM experiments were carried out to observe active mechanisms of this material during electrode operation.

2. Experimental

The *in situ* lithium-ion cell consisted of two electrodes and was designed in a way that allowed for the observation inside the SEM. The lower electrode was pure lithium metal and the working electrode which contained the material under investigation was placed on the top of the cell (Fig. 1). The working electrode had to be permeable for the electrolyte and therefore a stainless steel mesh (DIN 1.4401/AISI 316) was used as current collector. As in normal batteries, the electrode coating on this mesh was composed of the active material, polyvinylidene fluoride (PVDF) as a binder and carbon black for enhancing electronic conductivity. These materials were milled and mixed using mortar and pestle, and then several drops of N-methyl-2-pyrrolidone (NMP) were added to dissolve the PVDF binder. The slurry was then coated onto the stainless steel mesh and dried in air at room temperature for 24 h. Additional drying occurred in a furnace at 90 °C for another 24 h in order to remove the remaining NMP and minimize the water content. For the electrolyte, a 0.5 M solution of Li–bis(trifluoromethanesulfonyl)imide (Li–TFSI, conducting salt) in butylmethylpyrrolidinium–TFSI (BMPyrr–TFSI, ionic liquid, both generously provided by Ionic Liquid Technologies GmbH, Heilbronn, Germany) was used. The water content of the IL was investigated using coulometric Karl-Fischer titration and values below 120 ppm in the as delivered state and below 30 ppm in the additionally dried state were determined. Due to its very low vapor pressure, the ionic liquid solvent can be easily used inside the vacuum of the SEM chamber. Preliminary tests showed that this electrolyte is even compatible with ultra high vacuum (pressures below 10^{-8} mbar). As a separator, a laboratory filter paper (100% borosilicate glass microfibre, Whatman GF/B) was used.

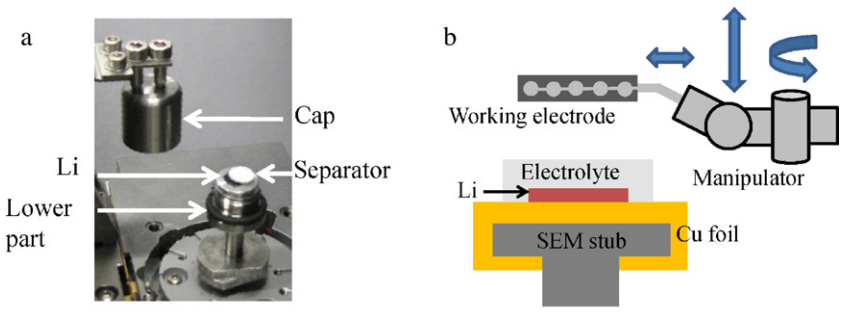

Fig. 2. (a) Home-built transfer system (opened) containing the lower part of the cell. The container can be opened by removing the cap inside the SEM chamber under high vacuum. (b) Inside the SEM, the electrode under investigation is placed onto the separator.

Several steps were needed to assemble the test cell. The lower part was assembled inside a glove box under protective argon atmosphere and the upper part containing the working electrode was placed on top of separator inside the SEM. For the lower part, a standard SEM stub made from aluminum was covered by a thin copper foil in order to make it electrochemically compatible with lithium. After that, a small piece of lithium was mounted onto this copper foil and the separator was placed on top of it and soaked by a few drops of the IL based electrolyte. After this step, the lower part of the cell was ready for transfer to the SEM. Since it contained the electrolyte and elementary lithium, it had to be protected from the atmosphere during transfer. For this purpose a home-built transfer system was used. It consists of a small container that hermetically enclosed the lower part of the test cell (Fig. 2a) and was mounted into the SEM chamber. After the chamber of the SEM was pumped to $\sim 10^{-5}$ mbar, the container was opened. The home-built system could be opened and closed using the motion and rotation of the SEM stage. Instead of this system, commercial load lock based transfer systems may be used. For further assembly of the battery inside the SEM, the working electrode had to be placed on top of the separator. This was done using a micromanipulator (Kleindiek MM3A-EM, Kleindiek GmbH, Reutlingen, Germany) (Fig. 2b). The steel mesh was clamped to the manipulator and therefore the manipulator also provided the electrical contact to the working electrode. The other electrical contact to the counter electrode was established through the SEM chamber and the conventional electrical grounding of the SEM. Assembling the cell in this two stage process proved to be very useful because it was possible to monitor and control the wetting of the working electrode by the electrolyte by carefully pushing it towards the separator using the manipulator (Fig. 3a).

The observation of the cell inside the SEM is complicated by the fact that electrons are involved in imaging. Typical electron beams used in SEMs have currents on the order of 1 nA. During scanning, this beam hits a very small area of a few nm^2 and can therefore lead to significant charging of the imaged region. In the battery such effects can strongly interfere with battery operation and therefore have to be prevented. Most problematic in this respect is the electrolyte which is by design a poor electron conductor. When imaged in the SEM, it can strongly build up charge leading to unwanted effects like local lithium deposition. For imaging, it is therefore important to select regions of the battery that have both, a good electronic connection to the current collector and are not covered by large amounts of electrolyte. Typically, regions close to the stainless steel mesh (Fig. 3b) were selected and beam currents and imaging times were minimized to avoid charging effects. The *in situ* batteries were electrically cycled using a computer controlled (Labview TM) current source/sink (Keithley 2400 sourcemeter). Depending on the materials investigated and

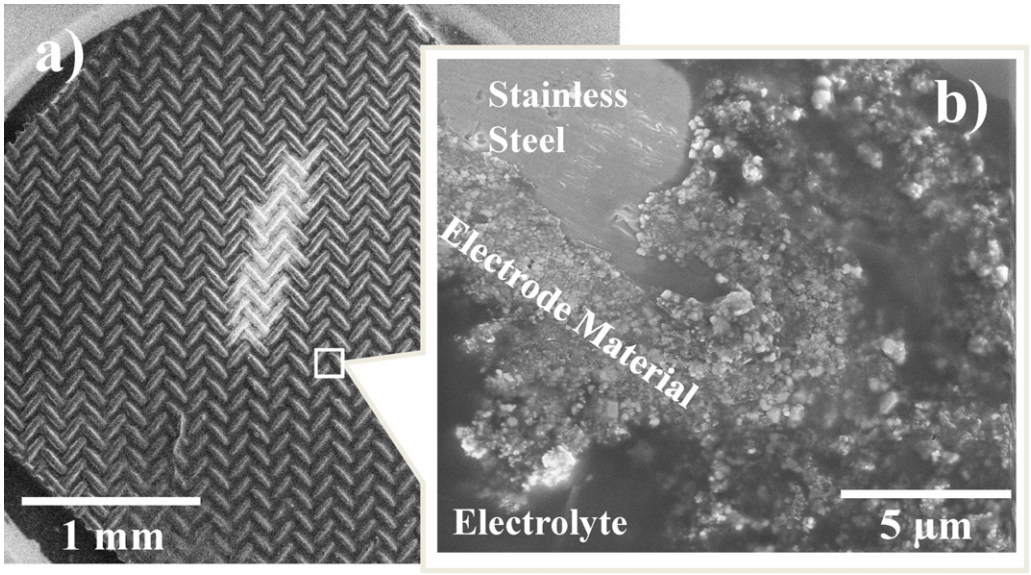

Fig. 3. SEM image taken during battery assembly. Using the manipulator, the working electrode is pushed towards the separator so that it is soaked in the electrolyte leading to the darker region in the image (a). Once fully soaked, regions very close to the stainless steel mesh (b) were selected for imaging to ensure proper grounding and to avoid electric charging effects.

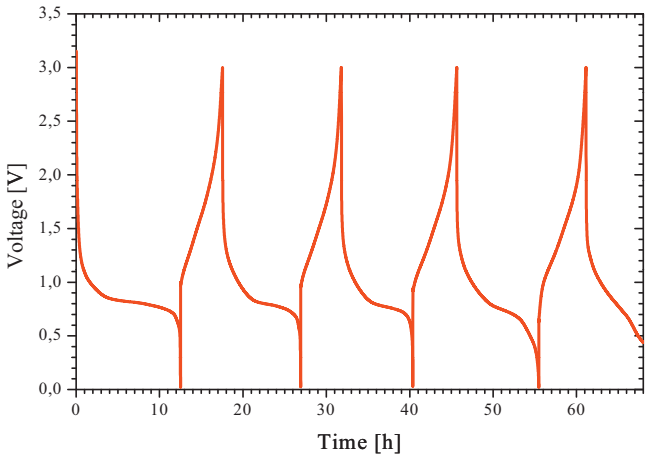

Fig. 4. Galvanostatic charge/discharge curves of SnO_2. The material was cycled between 0.02 V and 3 V against a lithium metal counter electrode.

size of the electrodes, currents for the small batteries were in the range between 100 nA and several 10 μA.

First experiments with this method were performed on SnO_2. SnO_2 powder (Sigma–Aldrich) with 99.9% purity and −325 mesh was used. The size distribution of the particles in the electrodes was very broad with diameters ranging from tens of nanometers to several micrometers. The electrodes contained 10 wt.% carbon black and 10 wt.% PVDF.

3. Results

During electrochemical cycling under constant current between 0.02 V and 3 V (Fig. 4), the top electrode could be imaged in real time. Several effects could be identified by monitoring different locations of the electrode. The effects that are presented here have been repeatedly observed so that it can be assumed that these observations are representative for what is occurring inside the electrode. During discharge, when lithium was inserted into the SnO_2, irreversible changes on the surface of the electrode particles occurred. No changes in the electrode were observed during delithiation.

A region of the electrode containing small particles with dimensions below 100 nm is shown in Fig. 5. It may be assumed that the changes in volume are more or less isotropic so that the three-dimensional volume changes can be estimated from the two-dimensional area changes. Upon the first insertion of lithium into the SnO_2 particles, the volume of the particles increased dramatically. The smallest particles showed volume changes of more than one order of magnitude. The increase in particle size occurred within the first few cycles with the change that happened within the first cycle being the largest one. At times when lithium was extracted, no growth or shrinkage could be seen. Depending on imaging conditions, brighter and darker regions could be identified on the particles. During the first few cycles, the darker shell increased in thickness and then stabilized. The brighter part in the center of the particles slightly decreased in size over the course of several cycles.

On the larger particles, different observations were made. These particles also showed a strong increase in size as can be seen from Fig. 6. This increase was accompanied by a blurring of the edges and a rounding of the corners. Shells as observed on the smaller particles did not seem to form. Although the volume increase was significant, it was smaller than that of the

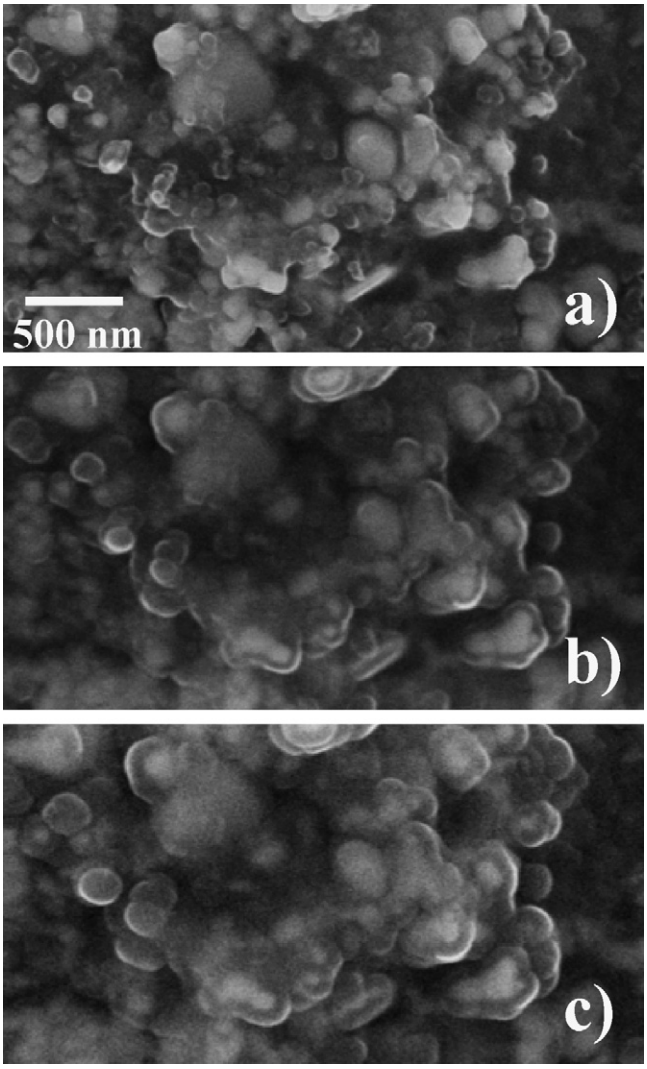

Fig. 5. SnO_2 particles at initial state (a), after first insertion of lithium (b) and after the second insertion (c). The images have the same magnification.

small particles as can be seen by comparing Fig. 5 with Fig. 6. This volume increase also was observed to be irreversible. In the larger particles, cracks were found quite frequently (Fig. 6) whereas no cracks were observed in the smaller particles. The growth of extrusions was often observed on the large particles (Fig. 7). In the SEM, the extrusions appeared to be brighter than the particles themselves. Formation of extrusions was only observed when lithium was inserted and when lithium was extracted no change of these extrusions could be seen. Almost all of the extrusions formed during the first half cycle where lithium was inserted and only few of them formed during later cycles. Although the observations that are presented here were made at the top of the electrode at regions that were not fully covered by the electrolyte (Fig. 3b), we have experimental evidence that the same or similar processes also occur underneath the electrolyte level. Thin layers of the electrolyte are electron transparent at high accelerating voltages. Although images taken at such conditions are blurred and the electrolyte strongly charges, it was possible to confirm that the described processes take place underneath the electrolyte level. For example, SEM observations performed at the end of the *in situ* experiment showed that extrusions also formed underneath the surface of the electrolyte.

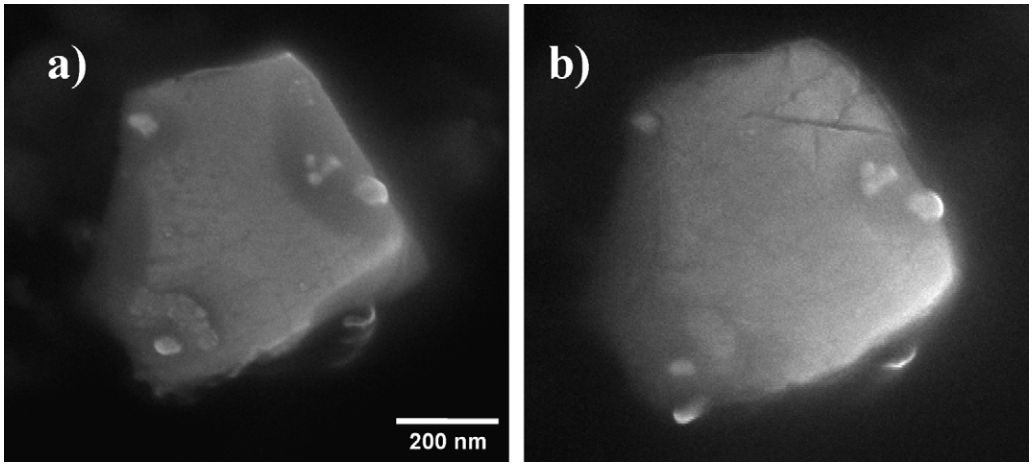

Fig. 6. Single SnO_2 particle before (a) and after the first lithium insertion (b). Besides the volume expansion, cracks and extrusions (lower left) appeared on the particle surface after the first lithium insertion.

4. Discussion

4.1. SnO_2

In the *in situ* SEM observations on the SnO_2 electrodes, microscopic morphological processes occurring in the electrodes have been identified. The overall electrochemical behavior of the electrode in Fig. 4, shows that during all cycles more lithium was inserted than was extracted. This is most likely due to an irreversible reaction of some of the lithium with the electrode. In the SEM observations, characteristic differences between small (Fig. 5) and large particles (Fig. 6) were found. As can be seen from Fig. 5, the small particles form layers on their surface. The images in Fig. 5 were taken at beam energies of 10 kV and contain not only secondary but also backscattered electrons. The number of backscattered electrons that are generated during imaging depends on the average atomic number Z of the material under investigation and therefore brighter regions correspond to elements with larger Z. Since the shells in the image appear darker than the particle themselves, it is very likely that these shells consist of Li_2O which has been proposed to form during the first lithium insertion [12]. The observations that were made here show that this process is not reversible, i.e. the shells do not shrink upon lithium extraction. The growth of the shells is not completed after the first cycle which is consistent with the data in Fig. 4. It was observed that the shell increased in thickness over several cycles when lithium was inserted. Inside the shells, brighter regions remain. These regions have shapes that are very similar to the initial particles. Over the course of three cycles, the thickness of the shells significantly increased and the brighter regions slightly decreased in size. This is consistent with the Li_2O formation where the loss in oxygen from the SnO_2 causes a small volume change in the $Sn + SnO_2$ particle and a large volume change in the Li_2O which is an amorphous low density material. The results indicate that the small SnO_2 particles with dimensions on the order of 100 nm form a layer of Li_2O that completely encapsulates the particle as a whole. The volume expansion in this system is solely caused by the formation of the shells and only little volume change in the form of particle shrinkage occurs in the core of this composite system. No defects in the form of cracks or extrusions were detected on the small particles. It seems that the core–shell composite that formed is effective in limiting the expansion of the particles.

Particles with dimensions larger than a few hundred nanometers behave differently than their smaller counterparts. In these particles the formation of surface layers was not observed (Fig. 6). Instead, the edges of the particles became rounded and the particle as a whole significantly increased in its size. The difference in behavior between small and large particles could be caused by the longer diffusion distances that are needed to bring the oxygen to the surface. For a given rate of cycling, there may be a critical particle size where either oxygen or Li_2O will not reach the surface of the particle anymore and where a different behavior is observed.

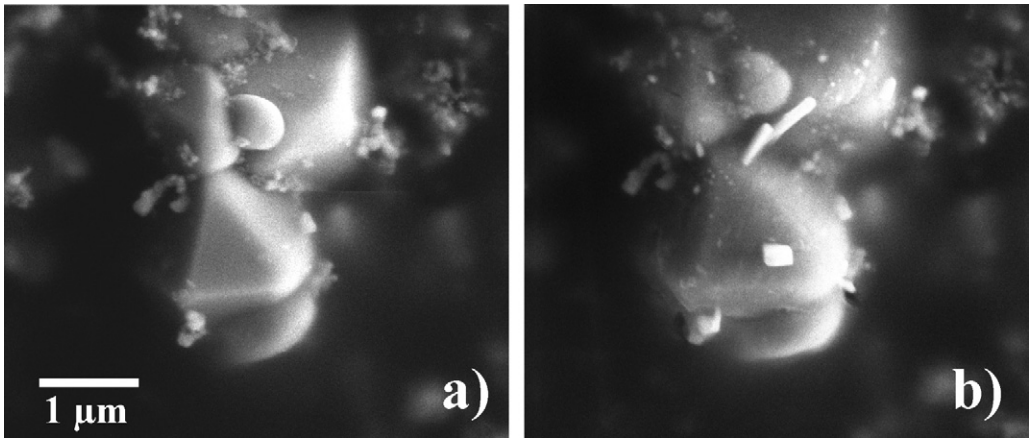

Fig. 7. SnO_2 particles in initial state (a) and after the first lithium insertion (b). Besides the significant volume expansion and extrusion formation, the edges of the particles became blurred.

Unfortunately, such effects can only be clearly identified by running experiments at different rates which was not performed in this study. Assuming an isotropic expansion, the particle in Fig. 6 increased in volume more than 50%. Larger particles that were also observed showed similar or slightly smaller amounts of expansion than the particle in Fig. 6. When comparing the SnO_2 particle in Fig. 6a with the particle in Fig. 6b it can be seen that although the volume expansion is visible, the appearance and shape of the particle surface did not change. This is surprising, since the amount of SnO_2 that is available in the particle must be conserved. If the particle still consists of SnO_2, strains on the order of 15% are required for a volume expansion by a factor of 1.5. Assuming an elastic modulus of 100 GPa [14] this would result in a very high tensile stress of 15 GPa. It is not very likely that the particle can withstand such high stresses since it most likely contains defects (e.g. surface irregularities, edges, etc.) that may serve as nucleation sites for cracks. It is therefore quite likely that the particle either consists of a material other than SnO_2 or that it is a mixture containing both SnO_2 plus an additional phase. For the case that the second phase is finely intermixed with the SnO_2, it may not be detectable by SEM. Concerning the mechanical stresses; there are clear indications that there are high tensile stresses in the large particles since cracks were commonly found. Also extrusions were frequently observed to form on the large particles. The mechanism responsible for the growth of extrusions can be complex and in many cases is not understood but in many systems compressive stresses are responsible for extruding the material. Fig. 7 shows an example where extrusions grew on a particle. In the SEM images the extrusions appear to be brighter and therefore may be composed of Sn or the Sn–Li alloy that is expected to form. In the course of cycling, it was observed that extrusions formed when the lithium was inserted into the SnO_2. The number of extrusions increased with the number of cycles. Some of the extrusions or whiskers grew in size with the number of cycles, other remained unchanged and new extrusions were observed to form in every cycle. The fact that extrusions form on the larger particles suggests that the chemical reactions are inhomogeneous and occur internally whereas on the small particles protective shells form during their reaction with lithium. The fact that the large particles often contain defects in the form of cracks and extrusions suggests that electrodes made from coarse particles are less reliable than electrodes containing small particles with sizes of 100 nm or below. This is also supported by electrochemical measurements [13,15].

4.2. In situ SEM

As can be seen from the results presented here, the method that has been described for *in situ* SEM studies on battery electrodes can be successfully used to investigate microscopic effects in electrochemical reactions. The use of an ionic liquid based electrolyte allows performing experiments under high vacuum. Experiments can be performed inside a conventional SEM where higher spatial resolutions can be achieved than in environmental or variable pressure microscopes. Sample transfer under protective atmosphere and the availability of electrical contacts inside the SEM are of critical importance for this method. Imaging battery materials inside the SEM can be difficult since high beam energies and high current densities are applied to the battery. In order to produce realistic results, care has to be taken to identify and if necessary to minimize the effect of the electron beam on the electrode material. This is particularly the case for the *in situ* experiments which contain an electrolyte and a counter electrode. When imaging, the battery can either charge positively or negatively depending on the number of electrons that are produced per incoming electron. Depending on the local electronic conductivity of the battery this can lead to unwanted electrochemical reactions. Such effects can be estimated by imaging the battery while keeping it at constant electrochemical potential. Only when no changes in the material occur, it can be assumed that the system is not affected by the SEM observation. In order to avoid such effects, a proper electronic connection of the electrode material to the current collector (mesh) has to be ensured and suitable regions have to be selected for imaging. Optimizing the beam energy (often low voltages help) and using very low beam currents in combination with infrequent monitoring may help to perform experiments even on sensitive and poorly electron conducting systems. A critical issue is the electrolyte itself. It is designed not to be electron conducting and therefore the direct imaging of the electrolyte may lead to local lithium deposition or charging. It was observed that charged regions on the liquid electrolyte react by coulomb interaction with each other and lead to unwanted motion of the electrolyte and a local flooding of the electrode. Although there are the aforementioned drawbacks associated with this method, it offers the unique opportunity to watch a working electrode in real time with very high resolution. Such experiments are useful for revealing the microscopic mechanisms caused by chemical reactions in conversion materials as was demonstrated here for the case of SnO_2.

5. Summary

A novel experimental platform was developed for the *in situ* SEM investigation of electrodes for lithium-ion batteries. It uses an ionic liquid based electrolyte which allows the operation of a special battery under vacuum. With this it is possible to observe a battery inside a SEM under high resolution. This concept could be possibly adapted to other investigation methods such as transmission electron microscopy or photoelectron spectroscopy. Using this method, experiments on SnO_2 were performed that reveal some of the active mechanisms in this material and show that the electrochemical behavior of this material strongly depends on particle size.

References

[1] M. Arakawa, et al., Journal of Power Sources 43 (1993) 27–35.
[2] T. Osaka, et al., Journal of Electroanalytical Chemistry 421 (1997) 153–156.
[3] Z. Takehara, et al., Journal of Power Sources 44 (1993) 377–383.
[4] D. Aurbach, Y. Gofer, J. Langzam, Journal of the Electrochemical Society 136 (1989) 3198–3205.
[5] T. Osaka, et al., Journal of the Electrochemical Society 144 (1997) 1709–1713.
[6] N.P.W. Langenhuizen, Journal of the Electrochemical Society 145 (1998) 3094–3099.
[7] P. Baudry, M. Armand, Solid State Ionics 28–30 (1988) 1567–1571.
[8] F. Orsini, et al., Journal of Power Sources 76 (1998) 19–29.
[9] P.R. Raimann, et al., Ionics 12 (2006) 253–255.
[10] J. Fuller, R.T. Carlin, R.A. Osteryoung, Journal of the Electrochemical Society 144 (1997) 3881–3886.
[11] A. Lewandowski, A. Swiderska-Mocek, Journal of Power Sources 194 (2009) 601–609.
[12] I.A. Courtney, J.R. Dahn, Journal of the Electrochemical Society 144 (1997) 2045–2052.
[13] J. Yang, M. Winter, J.O. Besenhard, Solid State Ionics 90 (1996) 281–287.
[14] S. Barth, et al., Nanotechnology 20 (2009) 11.
[15] Y.C. Chen, et al., Surface & Coatings Technology 202 (2007) 1313–1318.